Electronic Supplementary Information:

Hierarchical Organization in Liquid Crystal-in-Liquid Crystal Emulsions

Peter C. Mushenheim and Nicholas L. Abbott*

Department of Chemical and Biological Engineering, University of Wisconsin-Madison, 1415

Engineering Drive, Madison, WI, 53706, USA. Fax: +1 608-262-5434; Tel: +1 608-265-5278;

*Correspondence: abbott@engr.wisc.edu

Supplementary Text

Configurations of small 5CB droplets (diameters less than ~6 μm) dispersed in nematic DSCG

The internal configurations of 5CB droplets with diameters smaller than ~6 μm are difficult to determine when dispersed within the DSCG films (~60 μm in thickness) because the optical retardance of the DSCG ($\Delta n = -0.02$) film is comparable to or exceeds the optical retardance of the 5CB ($\Delta n = +0.18$) droplets with diameters less than ~6 μm. That is, the birefringence of the encompassing DSCG phase obscures the optical appearance of the small 5CB droplets (Fig. S3). We also note that nematic DSCG does not appear to adopt a twisted configuration around 5CB droplets less than ~6 μm in diameter (in agreement with the observations of Nych *et al.* of the alignment of nematic DSCG around isotropic droplets of this size[1]).

Theoretical estimates of root mean square displacement and angular deviation

We estimated diffusion coefficients for translational ($D_t = \frac{k_B T}{6\pi\eta R} \sim 0.002\ \mu m^2/min$) and rotational ($D_r = \frac{k_B T}{8\pi\eta R^3} \sim 0.05\ deg^2/min$)[2] motion of a spherical particle with R = 10 μm within nematic 15 wt% DSCG. In making these estimates, we note that we have neglected the anisotropy of the viscosity of the DSCG phase, and approximated it as an isotropic medium with an effective viscosity ($\eta \sim 0.7\ Pa\ s$)[3]. Using these diffusion coefficients, we arrived at theoretical estimates for the root mean square displacement in two dimensions ($\sqrt{\langle x^2 \rangle} = \sqrt{4D_t t} \sim 0.1\ \mu m$) and the root mean square angular deviation about a single axis ($\sqrt{\langle \phi^2 \rangle} = \sqrt{2D_r t} \sim 0.3°$) expected over one minute. These values are consistent with our experimental

measurements that a 5CB droplet with radius R ~ 10 µm translated at < 0.5 µm/min and rotated

at < 1°/min in the absence of convective flows within the nematic DSCG phase (Fig. S4).

Experimental measurement of θ

To determine the angle formed between the symmetry axis of 5CB/MBBA droplets in bipolar

configurations and the far-field nematic DSCG director (θ), we imaged the bipolar droplets (in

crossed polar and bright field modes) with the focal plane adjusted to the midplane of the

droplet. ImageJ software was used to determine the radius of the droplet, the position of the

center of the droplet, as well as the position of the projection of one of the boojums of the bipolar

droplet on the droplet's midplane in the bright field micrograph. Using trigonometry, the

locations of the boojums of the 5CB/MBBA droplet were determined from this information. The

orientation of the far-field director of the nematic DSCG phase was determined using the images

obtained through crossed polars and used to determine the locations of the boojums in the DSCG

phase at the surface of the droplets. Through knowledge of the positions of both the DSCG and

5CB/MBBA boojums, trigonometric relations could be employed to calculate θ.

Estimation of interfacial tension between 5CB and nematic DSCG phases

Our estimate of the interfacial tension between 5CB and the aqueous DSCG phase is based on

prior measurements of water-5CB interfacial tensions. We believe this estimate is reasonable

because DSCG is not amphiphilic. Specifically, at room temperature, an interfacial tension of

2.6×10^{-2} N/m was measured between 5CB and pure water[4] and an interfacial tension of 6×10^{-3} N/m was reported between 5CB and an aqueous solution containing 30 wt% $CaCl_2$ and 1 wt%

polyvinyl alcohol[5]. By approximating the interfacial energy of a 5CB droplet in nematic DSCG

(which scales as $\sim\gamma R^2$) as $\gamma \sim 10^{-3}$ N/m, and for 5CB droplets of R $\sim$ 10 μm, we estimate the interfacial energy ($\sim 10^{-13}$ J) to be much larger than the bulk elastic energies ($\sim 10^{-16}$ J). We note that if we instead used $\gamma \sim 10^{-2}$ N/m in our scaling argument, it would only serve to strengthen our conclusion that the interfacial energy of droplets of R $\sim$ 10 μm exceeds the bulk elastic energies.

Experimental test to determine if interactions with the polyimide alignment layer influence droplet relaxation

To determine if interactions involving the rubbed polyimide alignment layer contributed to the observed relaxation of the droplet orientations in our experiment, we applied a magnetic field parallel to the direction of rubbing to a dispersion of 5CB droplets in isotropic 98 wt% glycerol, which has a viscosity similar to nematic DSCG. The 5CB droplets were observed to reorient in the magnetic field, however, we did not observe the droplets to relax to an orientation orthogonal to the direction of rubbing (as was observed when the continuous phase was nematic DSCG (Fig. 3)) when the magnetic field was removed (Fig. S8).

Theoretical estimation of E_{aniso}

We calculated the orientation-dependent van der Waal's interaction between two semi-infinite planar slabs of uniformly aligned nematic 5CB and nematic DSCG. When the directors of both LCs are oriented parallel to the interface and at an angle θ relative to one another, and when the planar LC slabs are separated from one another at a distance d across an isotropic medium, the anisotropic part of the van der Waal's interaction can be evaluated as:

$$E_{aniso} = \frac{-kT}{64\pi d^2}\gamma_{5CB}\gamma_{DSCG}\cos^2\theta.[6]$$ In this expression, $\gamma_i = \frac{\sqrt{\varepsilon_\perp^i \varepsilon_\parallel^i}(\varepsilon_\perp^i - \varepsilon_\parallel^i)}{2\varepsilon_\parallel^i\left(\sqrt{\varepsilon_\perp^i \varepsilon_\parallel^i} + \varepsilon_m\right)}$, where $\varepsilon_\parallel^i$ and $\varepsilon_\perp^i$ are

the dielectric response functions parallel and perpendicular to the LC director, respectively,

which are related to the refractive indices of the LCs by $\varepsilon_\parallel \sim n_\parallel^2$ and $\varepsilon_\perp \sim n_\perp^2$. The dielectric

response of the isotropic medium, ε_m, is also related to the refractive index of the medium by

$\varepsilon_m \sim n_m^2$. Employing $n_\parallel = 1.71$ and $n_\perp = 1.53$ for 5CB[7] and $n_\parallel = 1.35$ and $n_\perp = 1.37$ for

DSCG (private communication from O. Lavrentovich), we calculate $E_{aniso} \sim 2 \times 10^{-7}\cos^2\theta$

J/m^2 for nematic 5CB and DSCG slabs separated by a thin layer (d = 0.2 nm) of water ($n_m = $

1.33). We note that we chose d = 0.2 nm in our calculation. However, the conclusions arising

from our calculation are not changed by using other values of d (e.g., d = 0.5 nm). If the two

slabs each have a surface area equal to the interfacial area of the droplet in Fig. 3 (the diameter of

the droplet was $\sim$ 24 µm), this estimate of E_{aniso} leads to the prediction that a change in the

relative orientation of the nematic directors of 5CB and DSCG from $\theta \sim 52°$ to $\theta \sim 74°$ results in

a lowering of the free energy of the system by $\sim 1 \times 10^{-16}$ J. This value is in close agreement

with the value obtained ($\sim 8 \times 10^{-17}$ J) via analysis of the dynamics of relaxation of the

orientations of a 5CB droplet following removal of an applied magnetic field (Fig. 3).

Supplementary References

1. A. Nych, U. Ognysta, I. Muševič, D. Seč, M. Ravnik, and S. Žumer, *Phys. Rev. E: Stat., Nonlinear, Soft Matter Phys.*, 2014, **89**, 062502.

2. R. B. Bird, W. E. Stewart, and E. N. Lightfoot, *Transport Phenomena*, John Wiley & Sons, New York, 2nd edn., 2007, p. 95-96.

3. P. C. Mushenheim, R. R. Trivedi, H. H. Tuson, D. B. Weibel, and N. L. Abbott, *Soft Matter*, 2014, **10**, 88-95.

4. J. E. Proust, E. Perez, and L. Ter-Minassian-Saraga, *Colloid Polym. Sci*, 1978, **681**, 666-681.

5. M. A. Gharbi, D. Seč, T. Lopez-Leon, M. Nobili, M. Ravnik, S. Žumer, and C. Blanc, *Soft Matter*, 2013, **9**, 6911-6920.

6. V. A. Parsegian, *Van der Waals Forces*, Cambridge University Press, Cambridge, 2005, p. 143.

7. L. M. Blinov and V. G. Chigrinov, *Electrooptic Effects in Liquid Crystal Materials*, Springer, New York, 1994, p. xiv.

Supplementary Figures
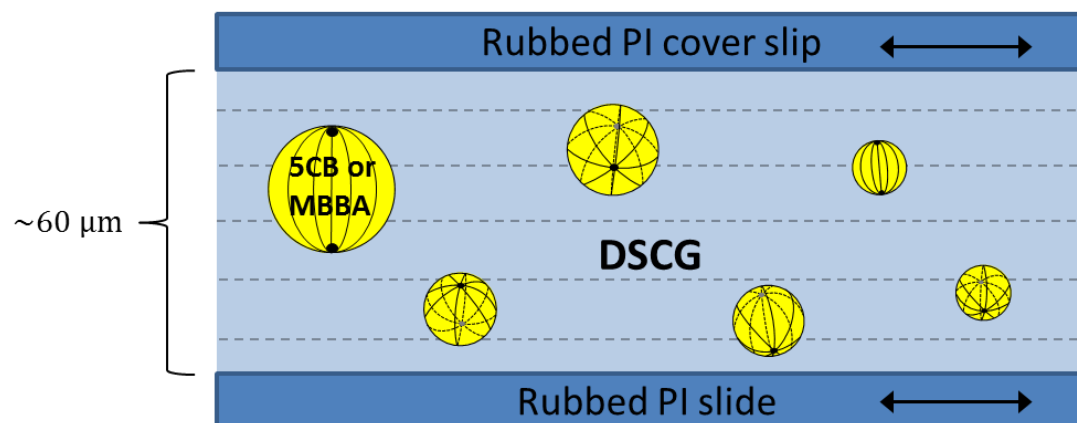
Fig. S1 Schematic illustration of the imaging chamber used to characterize LC-in-LC emulsions.

The double headed arrows indicate the direction of rubbing of the polyimide (PI) substrates.
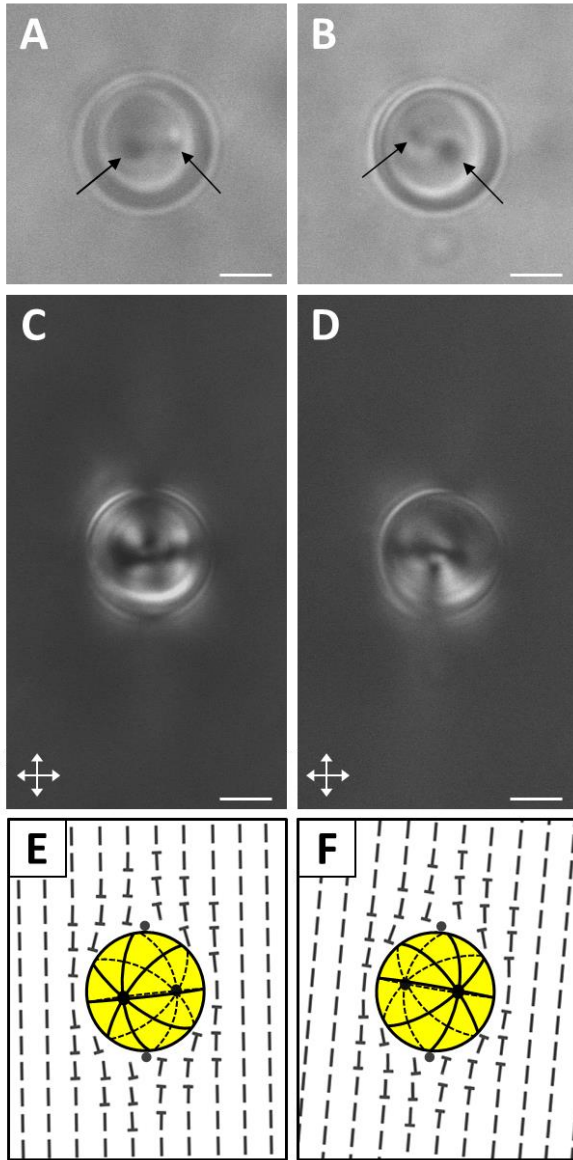
Fig. S2 Optical micrographs (A, B, bright field) and (C, D, crossed polars) of 5CB droplets with diameters of (A, C) 12.4 μm and (B, D) 12.0 μm. Both boojums (indicated by arrows) of the bipolar droplet configurations can be observed in A and B. (E, F) Corresponding schematic illustrations of the director profiles within the 5CB droplets as well as in the encompassing nematic DSCG. Scale bars = 5 μm.
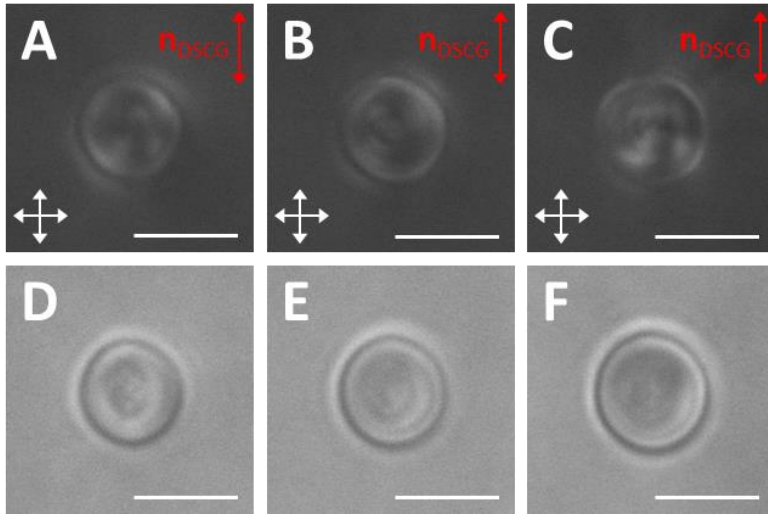
Fig. S3 Optical micrographs (A-C, crossed polars) and (D-F, bright field) of 5CB droplets with diameters of (A, D) 4.9 µm, (B, E) 5.1 µm, and (C, F) 5.4 µm dispersed within aligned regions of nematic DSCG. The far-field orientation of the DSCG is indicated in A-C. Scale bars = 5 µm.
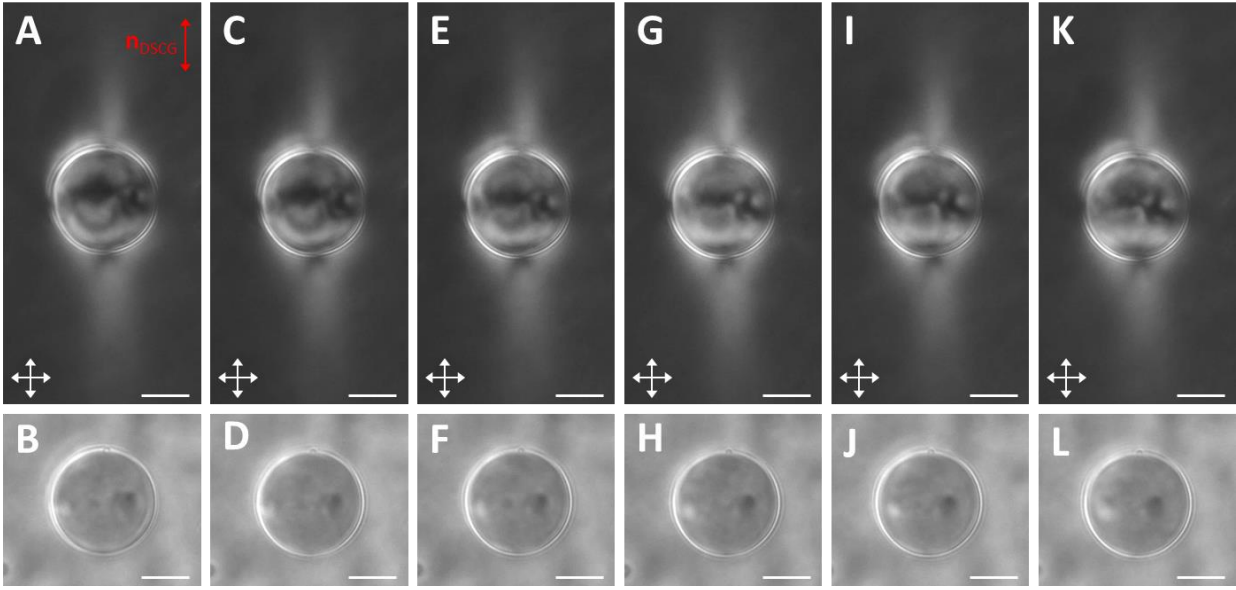
Fig. S4 Optical micrographs (A, C, E, G, I, K, crossed polars; B, D, F, H, J, L, bright field) of a 21.7 µm diameter nematic 5CB droplet suspended in nematic 15 wt% DSCG. Images acquired after (A, B) 0 min, (C, D) 3 min, (E, F) 6 min, (G, H) 9 min, (I, J) 12 min, and (K, L) 15 min. The far-field orientation of the DSCG is indicated in A. Scale bars = 10 µm.
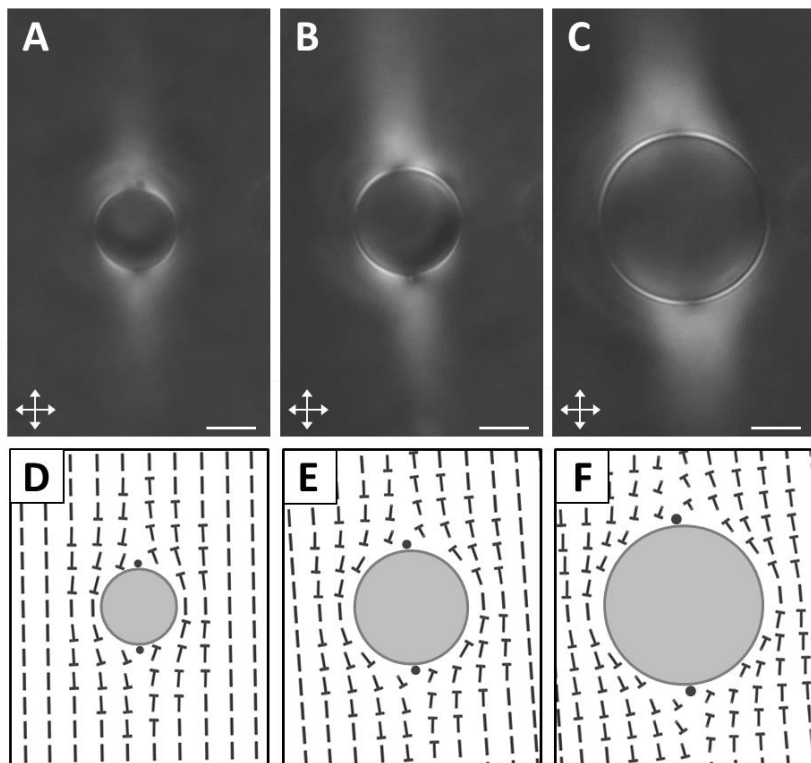
Fig. S5 Orientation of nematic 15 wt% DSCG near silicone oil droplets. (A-C) Optical micrographs (crossed polars) of silicone oil droplets with diameters of (A) 15.9 μm, (B) 21.3 μm, and (C) 33.5 μm. (D-F) Corresponding schematic illustrations of the director profiles in the nematic DSCG. Scale bars = 10 μm.
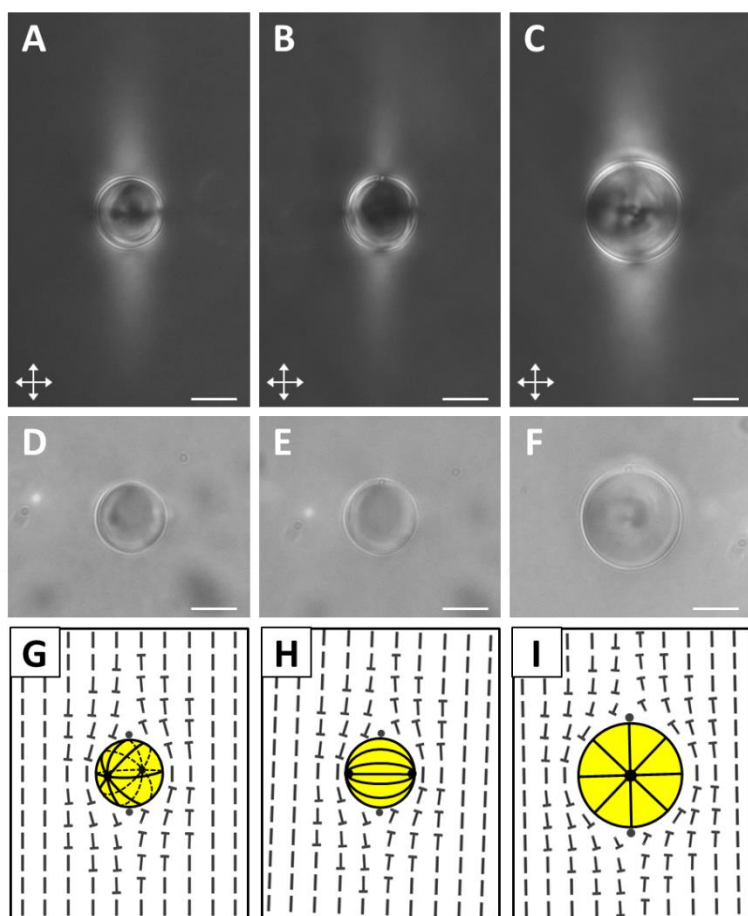
Fig. S6 Orientations of nematic MBBA emulsion droplets in nematic 15 wt% DSCG films. (A-F) Optical micrographs (A-C, crossed polars) and (D-F, bright field) of MBBA droplets with diameters of (A, D) 14.9 µm, (B, E) 15.6 µm, and (C, F) 21.2 µm. (G-I) Corresponding schematic illustrations of the director profiles within the MBBA droplets as well as in the encompassing nematic DSCG. Scale bars = 10 µm.
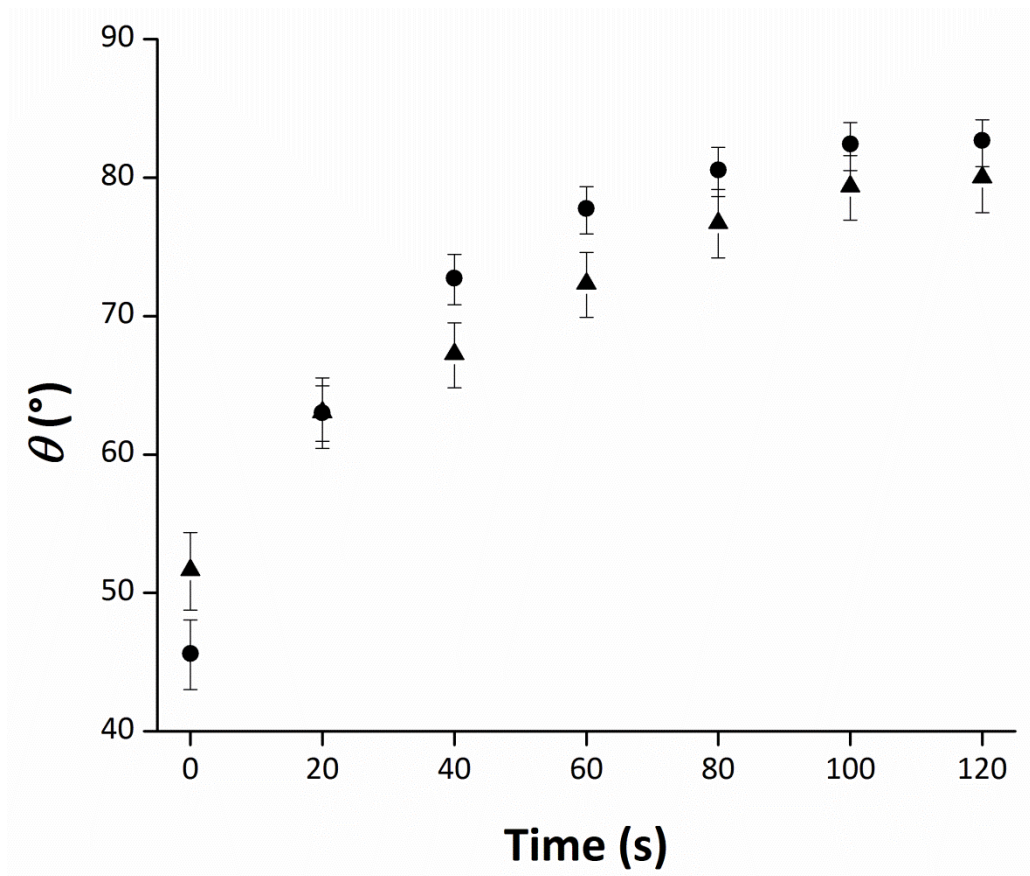
Fig. S7 Plot of the angle formed between the axis of symmetry of bipolar 5CB droplets (with diameters of 27.3 μm (●) and 23.6 μm (▲)) and to the far-field director of nematic DSCG (θ) as a function of time following removal of a magnetic field (**B** ~ 0.3 T) applied parallel to $\mathbf{n}_{DSCG}$ for 60s. Error bars represent uncertainty in the calculation of θ associated with estimating the positions of the 5CB droplet center and one of the boojums of the droplet.
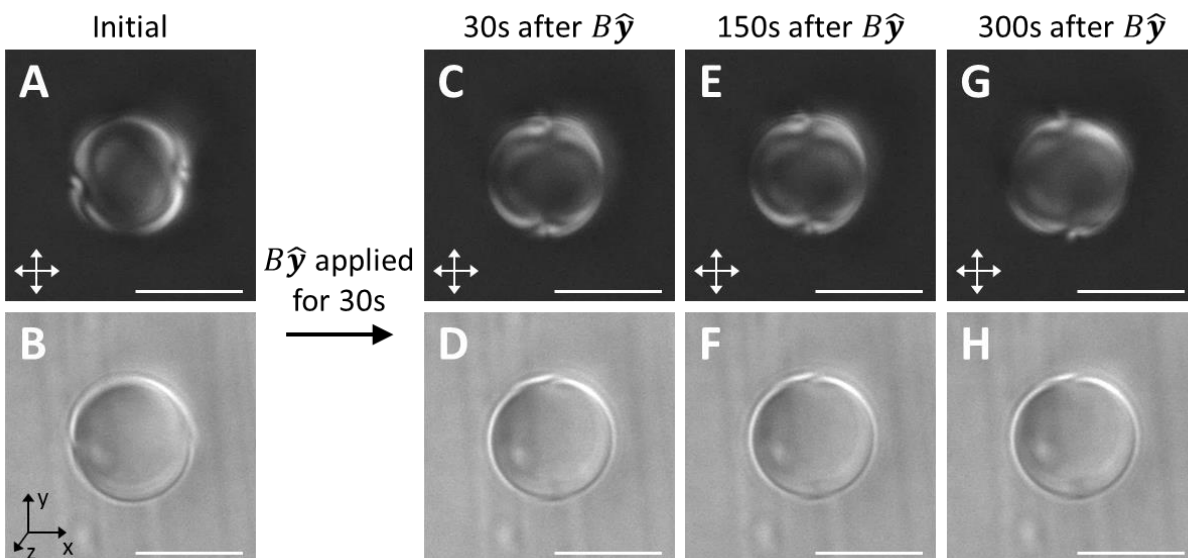
Fig. S8 Optical micrographs (crossed polars (A, C, E and G) and bright field (B, D, F and H)) of a nematic 5CB droplet dispersed within an isotropic 98 wt% DSCG solution between polyimide substrates both (A, B) before and (C-H) after application of a magnetic field ($\mathbf{B} \sim 0.3$ T). The magnetic field was applied in the $\hat{\boldsymbol{y}}$ direction (see coordinate system in B), parallel to the direction of rubbing of the polyimide substrate. The 5CB droplet is 11.2 μm in diameter. Scale bars = 10 μm.
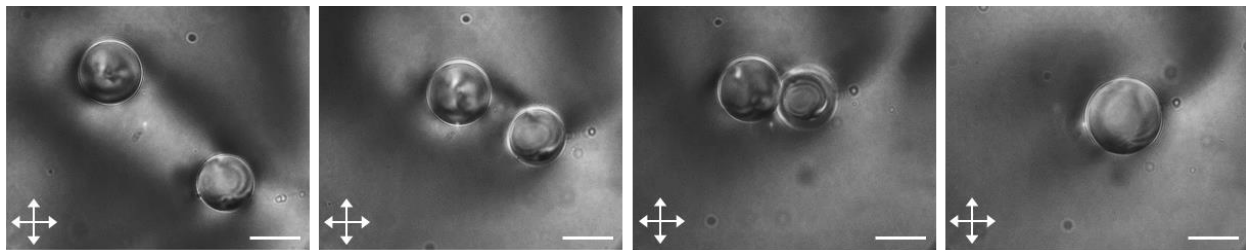
Fig. S9 Optical micrographs (crossed polars) showing the coalescence of two nematic 5CB droplets dispersed in a region of nematic DSCG that does not exhibit uniform azimuthal alignment. Scale bars = 20 μm.
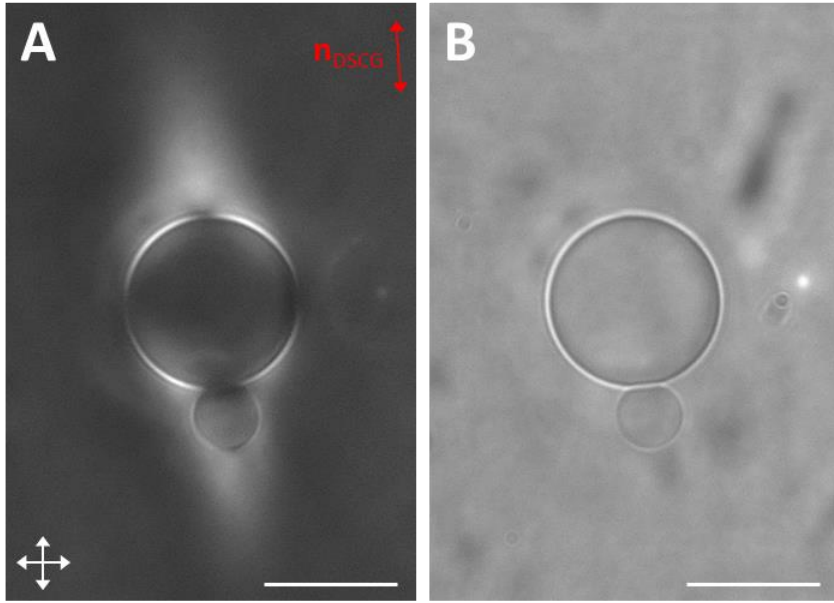
Fig. S10 (A, B) Optical micrographs (crossed polars, A and bright field, B) of two silicone oil droplets that adhered to one another within an aligned region of nematic DSCG. The far-field orientation of the nematic DSCG is indicated in A. Scale bars = 20 µm.
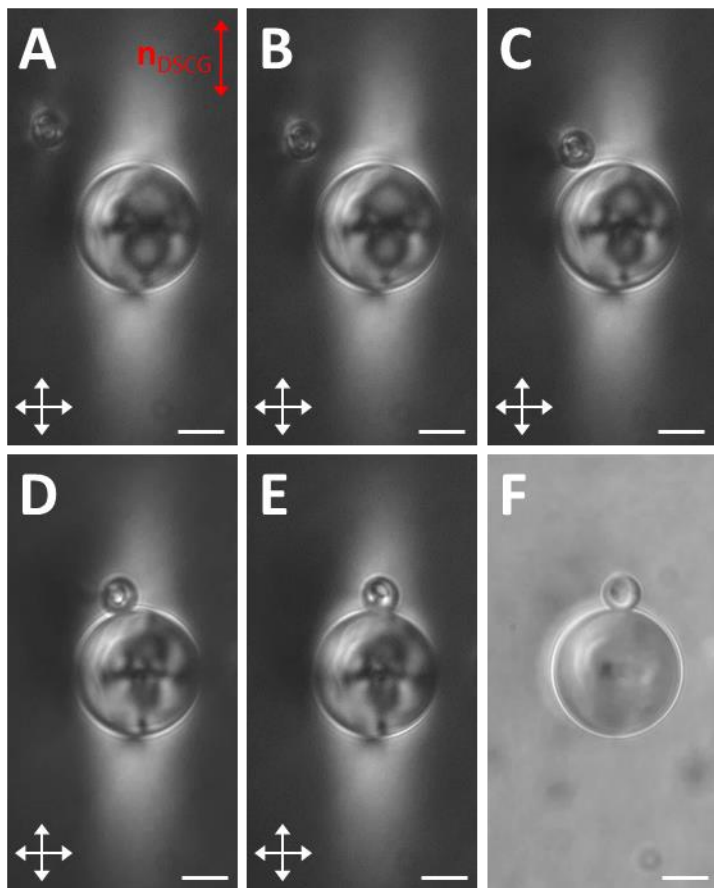
Fig. S11 Sequence of optical micrographs (crossed polars (A-E) and bright field (F)) showing the migration of a 7.9 μm diameter 5CB droplet within an aligned region of nematic DSCG to the DSCG boojum located near the surface of a 26.9 μm diameter 5CB droplet. The far-field orientation of the nematic DSCG is indicated in A. The micrographs were taken at (A) 0 min, (B) 5 min, (C) 10 min, (D) 13 min, (E) 16 min, and (F) 17 min. Scale bars = 10 μm.